Green Synthesis of New Category of Pyrano[3,2-c]Chromene-Diones Catalyzed by Nanocomposite as Fe3O4@SiO2-Propyl Covalented Dapsone-Copper Complex

Leila Zare Fekri *

Department of Chemistry, Payame Noor University, Tehran, Iran

Nanomagnetic dapsone-Cu supported on the silica-coated Fe_3O_4 (Fe_3O_4@SiO_2-pr@dapsone-Cu) nanocomposite was synthesized and characterized by Fourier transform infrared (FT-IR), energy-dispersive X-ray (EDX), X-ray diffraction (XRD), field emission scanning electron microscope (FE-SEM), transmission electron microscopy (TEM), zeta potential, vibrating sample magnetometer (VSM), and thermogravimetric analysis (TGA). This newly synthesized nanocomposite was chosen to act as a green, efficient, and recyclable Lewis acid for the multicomponent synthesis of new derivatives of pyrano[3,2-c] chromene-diones through the reaction of aromatic aldehydes, indandione, and 4-hydroxycoumarin in water. All of the synthesized compounds are new and are recognized by FT-IR, NMR, and elemental analysis; this avenue is new and has advantages such as short reaction times, high productivity, economical synthesis, and use of green solvent, H_2O, as a medium. The catalyst is magnetically recoverable and can be used after six runs without a decrease in the efficiency.

Keywords: dapsone-cu, silica-coated Fe3O4, silica, pyranochromenes, nanoorganometallic chemistry

INTRODUCTION

Multicomponent reactions (MCRs) are useful avenue for the synthesis of organic compounds. This reaction is a combination of at least three components in a one-pot domino (Li and Chan, 1997; Grieco, 1998; Dömling and Uzi, 2000; Dömling, 2002; Hosseini-Zare et al., 2012). MCRs have benefits such as higher atom economy and selectivity and production of complex molecules with low by-products. Nowadays, MCRs have attracted a lot of interest in organic transformation (Bienaymé et al., 2000; Kandhasamy and Gnanasambandam, 2009; Müller 2014).

Pyranochromenes have various biological activities such as antifungal (Ouf et al., 2014), antibacterial (Zhang et al., 2012), antihyperglycaemic and antidyslipidemic (Kumar et al., 2009), anticancer (Lee et al., 2009), cytotoxic (Magiatis et al., 1998), anti-HIV (Kongkathip et al., 2005), anti-HBV (Su et al., 2009), antiviral (Barnard et al., 2002), antiproliferative (Mao et al., 2019), anti-inflammatory (Symeonidis et al., 2009), antinociceptive (Lima et al., 2006), and antituberculosis (Xu et al., 2006). They are also synthetic intermediates for alkaloids, drug candidates, and clinical pharmaceuticals (Williams and Cox, 2003).

Magnetic nanoparticles (MNPs) as catalysts are interesting materials because of their high surface area, unique magnetic properties, and high catalytic activity. They were used as magnetic fluids

catalysis and magnetic resonance imaging (MRI) data storage and environmental remediation (Rezaee Nezhad et al., 2014; Mokhtary, 2016; Rezayati et al., 2016; Fekri and Maleki, 2017; Abbasi et al., 2017; Fekri et al., 2020; Sardarian et al., 2019; Inaloo et al., 2020a; 2020b; 2020c; 2020d).

To the best of our knowledge, there are no reports on the use of Fe3O4@SiO2-propyl-loaded dapsone-copper as a catalyst for the synthesis of pyrano[3,2-c]chromenes via multicomponent reactions of aldehydes, indandione, and 4-hydroxycoumarin results.

EXPERIMENTAL

Material and Method

The X-ray diffraction (XRD), transmission electron microscopy (TEM), scanning electron microscope (SEM), thermogravimetric analysis (TGA), and zeta potential analysis for synthesized MNPs were analyzed on X-PRTPRO (Netherlands) XRD, TEM Jeol model 3,010, Philips XL 30 scanning electron microscope (SEM), Netherlands), Q600 (made in America), and ZEN3600 (England) instrument, respectively. Fourier transform infrared (FT-IR) spectra of organic compounds were carried out by Shimadzu Fourier transform infrared spectrophotometer (FT-IR-470, Japan). 1H and 13C NMR spectra were determined using a Bruker DRX Avance instrument at 500 or 300 and 125 or 75 MHz.

General Procedure for Preparation of Fe_3O_4

Nanoparticles Fe_3O_4 were synthesized by Zare Fekri (Fekri and Maleki, 2017; Fekri, 2020).

Synthesis of Fe3O4@SiO2-Cl

$Fe_3O_4@SiO_2$ NPs were prepared by Zare Fekri (Nikpassand et al., 2017; Fekri et al., 2020; Fekri and Zeinali, 2020).

Synthesis of $Fe_3O_4@SiO_2@dapsone$

500 mg $Fe_3O_4@SiO_2$-Cl MNPs in 50 ml distilled water were irradiated under ultrasound for 30 min. Then, dapsone 0.5 g was added. The mixture was refluxed at 110°C for 14 h. The $Fe_3O_4@SiO_2@dapsone$ was filtered in the presence of an enormous magnet and washed with chloroform several times and dried at 80°C for 4 h.

Synthesis of $Fe_3O_4@SiO_2@dapsone-Cu$

500 mg $Fe_3O_4@SiO_2@dapsone$ MNPs in 50 ml EtOH-H_2O (1:1) were irradiated under ultrasonic bath for 30 min. Then, 20 ml aqueous solution of copper chloride (I) (0.1 g; 0.001 mol) was added to the $Fe_3O_4@SiO_2@dapsone$ and stirred for 48 h. The $Fe_3O_4@SiO_2@dapsone-Cu$ MNPs were filtered in the presence of a magnetic bar and washed using ethanol and water subsequently, to separate the nanoparticles.

General Procedure for the Synthesis of Pyrano[3,2-c]chromene-Dione

A mixture of aldehyde (1.0 mmol), indan-1,3-dione (2.0 mmol), 4-hydroxycoumarin (1 mmol), and 0.05 g $Fe_3O_4@SiO_2@$

dapsone-Cu MNPs was stirred at room temperature in 10 ml distilled water for the required reaction time as indicated by TLC (TLC silica gel 60 F250, ethyl acetate : n-hexane 1 : 4). After completion of the reaction, the resulting mixture was filtered in the presence of an efficient magnetic bar to separate the catalyst. The catalyst was washed with 10 ml ethanol and reused. The crude products were collected and dried.

Characterization Data

7-(4-Nitrophenyl)-6H-indeno [2',1':5,6]pyrano [3,2-c] chromene-6,8(7H)-dione 4a: m. p. 203–205°C, FT-IR (KBr, cm^{-1}): 1739 (C=O str), 1701 (C=O str), 1,561 (Asymmetric NO_2 str or aromatic C=C str), 1,510, 1,456 (aromatic C=C str), 1,348 (symmetric NO_2 str), 1,257 (C-O str), 1,099.^{1}H NMR (DMSO-d_6, 400 MHz): δ_H 5.31 (s, 1H, chiral C-H), 6.84–6.88 (m, 1H, Ar), 7.00–7.04 (m, 1H, Ar), 7.18 (d, J = 8.0Hz, 1H, Ar), 7.23 (d, J = 2.4Hz, 1H, Ar), 7.31 (d, J = 8.0Hz, 1H, Ar), 7.35 (s, 1H, Ar), 7.55 (d, J = 8.0Hz, 2H, Ar), 7.85–7.95 (m, 2H, Ar), 8.06–8.14 (m, 1H, Ar) ppm. ^{13}C NMR (DMSO-d_6, 100 MHz): δ_C 57.50 (chiral carbon), 111.60 (Ar), 113.45 (Ar), 117.89 (Ar), 121.98 (two peaks, Ar), 123.56 (Ar), 123.98 (Ar), 125.01 (Ar), 126.23 (Ar), 127.09 (Ar), 131.56 (Ar), 131.87 (Ar), 132.33 (Ar), 137.89 (Ar), 133.98 (Ar), 139.09 (two peaks, Ar), 141.23 (Ar), 145.81 (Ar), 149.87 (Ar), 198.76 (C=O), 201.17 (C=O)ppm. Anal. Calcd. for $C_{25}H_{13}NO_6$: C, 70.92; H, 3.09; N, 3.31. Found: C, 70.93; H, 3.05; N, 3.32.

7-(3-Nitrophenyl)-6H-indeno [2',1':5,6]pyrano [3,2-c] chromene-6,8(7H)-dione 4b: m. p. 176–177°C, FT-IR (KBr, cm^{-1}): 1736 (C=O str), 1700 (C=O str), 1,660, 1,580 (asymmetric NO_2 or aromatic C=C str), 1,430 (aromatic C=C str), 1,330 (symmetric NO_2 str), 1,275 (C-O str). ^{1}H NMR (DMSO-d_6, 400 MHz): δ_H 5.33 (s, 1H, chiral C-H)), 6.85 (t, J = 7.2Hz, 1H, Ar), 7.00 (t, J = 7.2Hz, 1H, Ar), 7.22 (d, J = 8.4Hz, 2H, Ar), 7.31 (d, J = 8.4Hz, 1H, Ar), 7.35 (d, J = 2.0Hz, 1H, Ar), 7.52 (t, J = 8.0Hz, 1H, Ar), 7.78 (d, J = 8.0Hz, 1H, Ar), 7.85–7.94 (m, 2H, Ar), 8.00–8.02 (m, 1H, Ar), 8.18 (d, J = 2.0Hz, 1H, Ar) ppm. ^{13}C NMR (DMSO-d_6, 100 MHz): δ_C 58.30 (chiral C), 112.00 (two peaks, Ar), 113.54 (Ar), 114.00 (Ar), 118.96 (Ar), 119.18 (Ar), 121.80 (Ar), 122.03 (Ar), 123.29 (Ar), 123.33 (Ar), 124.75 (Ar), 126.61 (Ar), 129.98 (two peaks, Ar), 135.84 (Ar), 136.36 (Ar), 136.66 (Ar), 142.40 (Ar), 142.44 (Ar), 144.60 (Ar), 147.91 (Ar), 198.90 (C=O), 200.16 (C=O) ppm. Anal. Calcd. for $C_{25}H_{13}NO_6$: C, 70.92; H, 3.09; N, 3.31. Found: C, 70.95; H, 3.07; N, 3.36.

7-(4-Bromophenyl)-6H-indeno [2',1':5,6]pyrano [3,2-c] chromene-6,8(7H)-dione 4c: m. p. 276–278°C, FT-IR (KBr, cm^{-1}): 1735 (C=O str), 1700 (C=O str), 1,650, 1,457 (aromatic C=C str), 1,215 (C-O str). ^{1}H NMR (DMSO-d_6, 400 MHz): δ_H 5.13 (s, 1H, chiral C-H), 6.85 (t, J = 7.2Hz, 1H, Ar), 7.01 (t, J = 7.2Hz, 1H, Ar), 7.13 (d, J = 8.0Hz, 1H, Ar), 7.17 (d, J = 8.4Hz, 2H, Ar), 7.31 (dd, J = 3.2Hz, J = 5.6Hz, 2H, Ar), 7.35 (dd, J = 1.6Hz, J = 6.4Hz, 2H, Ar), 7.84–7.93 (m, 2H, Ar) ppm. ^{13}C NMR (DMSO-d_6, 100 MHz): δ_C 58.48 (chiral C), 111.91 (Ar), 114.32 (Ar), 118.95 (Ar), 119.00 (Ar), 119.99 (Ar), 121.60 (Ar), 123.25 (Ar), 124.76 (Ar), 126.71 (two peaks, Ar), 131.06 (Ar), 131.21 (Ar), 131.27 (Ar), 136.44 (Ar), 136.54 (Ar), 136.58 (Ar), 141.35 (Ar), 142.38 (Ar), 142.61 (Ar), 144.32 (Ar), 197.56 (C=O), 200.26

SCHEME 1 | Multistep synthesis of Fe₃O₄@SiO₂-propyl@dapsone-Cu complex.
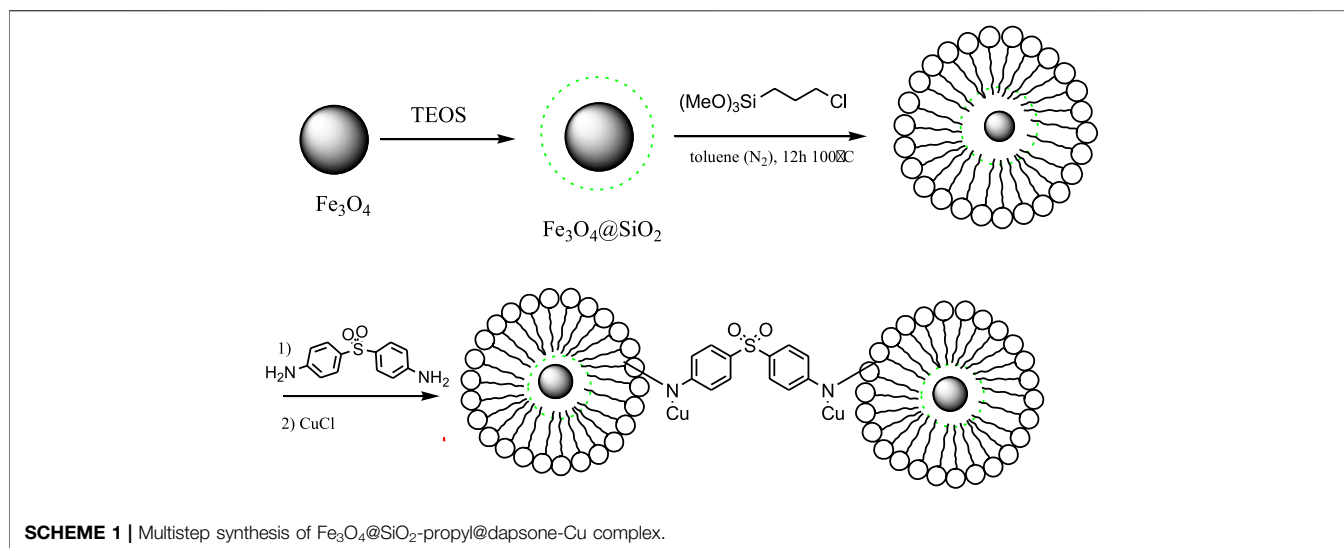
(C=O) ppm. Anal. Calcd. for $C_{25}H_{13}BrO_4$: C, 65.66; H, 2.87. Found: C, 65.65; H, 3.07; N, 2.86.

7-(3-Hydroxyphenyl)-6H-indeno [2',1':5,6]pyrano [3,2-c] chromene-6,8(7H)-dione 4d: m. p. 289–290°C, FT-IR (KBr, cm⁻¹): 1737 (C=O str), 1705 (C=O str), 1,650, 1,608 (aromatic C=C str), 1,538, 1,224 (C-O str). ¹H NMR (DMSO-d6, 400 MHz): δ_H 5.04 (s, 1H, chiral C-H), 6.41–6.44 (m, 1H, Ar), 6.57 (t, J = 7.8Hz, 1H, Ar), 6.92 (d, J = 8.7Hz, 1H, Ar), 6.84 (t, J = 8.5Hz, 1H, Ar), 6.90 (t, J = 8.5Hz, 1H, Ar), 7.00–7.04 (m, 1H, Ar), 7.14 (d, J = 8.5Hz, 1H, Ar), 7.32 (d, J = 7.8Hz, 1H, Ar), 7.41 (d, J = 4.3Hz, 1H, Ar), 7.83–7.92 (m, 3H, Ar), 9.13 (s, 1H, OH) ppm. ¹³C NMR (DMSO-d6, 100 MHz): δ_C 58.71 (chiral C), 111.83 (Ar), 113.91 (two peaks, Ar), 115.11 (Ar), 116.07 (Ar), 118.86 (two peaks, Ar), 118.99 (Ar), 119.63 (Ar), 121.48 (Ar), 123.15 (two peaks, Ar), 124.78 (Ar), 126.94 (Ar), 129.23 (Ar), 136.36 (two peaks, Ar), 136.43 (Ar), 142.45 (Ar), 142.85 (two peaks, Ar), 143.06 (Ar), 157.23 (Ar), 197.83 (C=O), 200.51 (C=O) ppm. Anal. Calcd. for $C_{25}H_{14}O_5$: C, 76.14; H, 3.58. Found: C, 76.11; H, 3.07.

7-(4-(Methylthio)phenyl)-6H-indeno [2',1':5,6]pyrano [3,2-c] chromene-6,8(7H)-dione 4e: m. p. 269–270°C, FT-IR (KBr, cm⁻¹): 2,921 (aliphatic C-H str), 1735 (C=O str), 1701 (C=O str), 1,593 (aromatic C = c str), 1,488 (aromatic C=C str), 1,423, 1,344, 1,261 (C-O str). ¹H NMR (DMSO-d₆, 400 MHz): δ_H 2.43 (s, 3H, SCH₃), 5.10 (s, 1H, chiral C-H), 6.84 (t, J = 7.8Hz, 1H, Ar), 7.01 (d, J = 8.5Hz, 3H, Ar), 7.13 (d, J = 8.5Hz, 3H, Ar), 7.31 (d, J = 3.2Hz, 1H, Ar), 7.36 (s, 1H, Ar), 7.86–7.92 (m, 2H, Ar) ppm. ¹³C NMR (DMSO-d6, 100 MHz): δ_C 51.63 (SCH₃), 58.75 (chiral C), 112.98 (Ar), 113.93 (two peaks, Ar), 114.01 (Ar), 115.08 (Ar), 116.81 (Ar), 117.23 (Ar), 119.53 (Ar), 120.56 (Ar), 122.05 (two peaks, Ar), 124.89 (Ar), 125.34 (Ar), 125.87 (Ar), 134.21 (Ar), 136.42 (Ar), 143.21 (two peaks, Ar), 145.17 (Ar), 158.23 (Ar), 196.23 (C=O), 201.01 (C=O) ppm. Anal. Calcd. for $C_{26}H_{16}O_4S$: C, 73.57; H, 3.80. Found: C, 73.51; H, 3.87.

7-(Pyridin-3-yl)-6H-indeno [2',1':5,6]pyrano [3,2-c] chromene-6,8(7H)-dione 4f: m. p. >300°C, FT-IR (KBr, cm⁻¹): 3,034 (aromatic C-H str), 2,910 (aliphatic C-H str), 1743 (C=O str), 1703 (C=O str), 1,565 (aromatic C=C str), 1,425 (aromatic

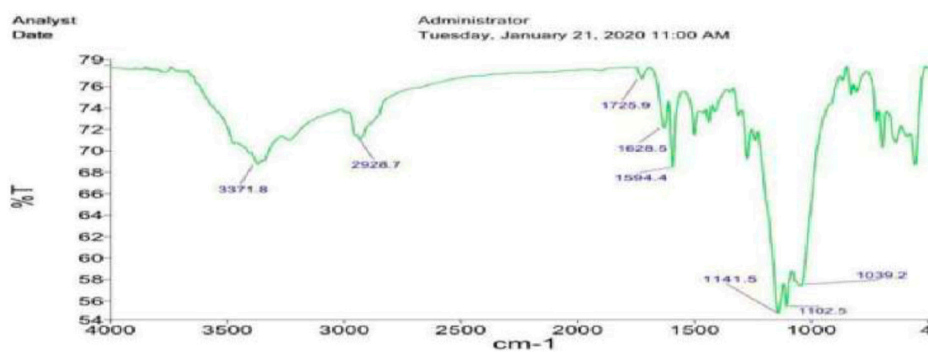C=C str), 1,265 (C-O str), 1,168. ¹H NMR (DMSO-d₆, 400 MHz): δ_H 5.21 (s, 1H, chiral C-H), 6.86 (t, J = 7.8Hz, 1H, Ar), 7.02 (t, J = 7.5Hz, 1H, Ar), 7.18–7.22 (m, 2H, Ar), 7.30 (t, J = 8.5Hz, 3H, Ar), 7.65 (d, J = 8.6Hz, 1H, Ar), 7.87–7.94 (m, 3H, Ar), 8.31 (d, J = 7.8Hz, 1H, Ar) ppm. ¹³C NMR (DMSO-d₆, 100 MHz): δ_C 56.78 (chiral C), 113.09 (two peaks, Ar), 114.56 (Ar), 116.12 (Ar), 116.91 (Ar), 116.99 (Ar), 118.13 (Ar), 118.76 (Ar), 121.43 (two peaks, Ar), 122.16 (two peaks, Ar), 123.54 (Ar), 125.57 (Ar), 126.47 (Ar), 128.46 (Ar), 134.09 (Ar), 138.11 (two peaks, Ar), 147.87 (Ar), 155.08 (Ar), 197.34 (C=O), 200.07 (C=O) ppm. Anal. Calcd. for $C_{24}H_{13}NO_4$: C, 75.98; H, 3.45; N, 3.69. Found: C, 75.93; H, 3.43, N, 3.65.

7-Phenyl-6H-indeno [2',1':5,6]pyrano [3,2-c]chromene-6,8(7H)-dione 4 g: m. p. 203–205 °C, FT-IR (KBr, cm⁻¹): 3,098 (aromatic C-H str), 1735 (C=O str), 1702 (C=O str), 1,603 (aromatic C=C str), 1,408, 1,365, 1,323, 1,211 (C-O str). ¹H NMR (DMSO-d₆, 400 MHz): δ_H 5.10 (s, 1H, chiral C-H), 6.35–6.56 (m, 3H, Ar), 6.68 (d, J = 7.8Hz, 2H, Ar), 6.86 (s, 1H, Ar), 6.98–7.11 (m, 2H, Ar), 7.28 (d, J = 6.8Hz, 3H, Ar), 7.34 (d, J = 8.2Hz, 2H, Ar) ppm. ¹³C NMR (DMSO-d₆, 100 MHz): δ_C 58.52 (chiral C), 114.23 (Ar), 114.38 (Ar), 116.01 (Ar), 116.98 (Ar), 117.45 (Ar), 117.67 (Ar), 117.89 (Ar), 121.32 (Ar), 121.67 (Ar), 123.55 (Ar), 124.78 (Ar), 126.98 (Ar), 127.46 (Ar), 129.00 (Ar), 132.65 (two peaks, Ar), 136.89 (Ar), 138.91 (Ar), 141.24 (Ar), 143.67 (Ar), 196.34 (C=O), 200.32 (C=O) ppm. Anal. Calcd. for $C_{25}H_{14}O_4$: C, 79.36; H, 3.73. Found: C, 79.31; H, 3.77.

7-(p-Tolyl)-6H-indeno [2',1':5,6]pyrano [3,2-c]chromene-6,8(7H)-dione 4h: m. p. 234–235°C, FT-IR (KBr, cm⁻¹): 1734 (C=O str), 1701 (C=O str), 1,576 (aromatic C=C str), 1,435 (aromatic C=C str), 1,387, 1,234 (C-O str), 1,114. ¹H NMR (DMSO-d₆, 400 MHz): δ_H 2.35 (s, 3H, Ph-CH₃), 5.31 (s, 1H, chiral C-H), 6.87 (d, J = 7.8Hz, 2H, Ar), 6.87–7.09 (m, 2H, Ar), 7.23 (J = 8.5Hz, 1H, Ar), 7.56 (d, J = 7.8Hz, 2H, Ar), 7.67–7.83 (m, 3H, Ar), 8.01–8.09 (m, 2H, Ar) ppm. ¹³C NMR (DMSO-d₆, 100 MHz): δ_C 34.23 (benzylic carbon), 58.65 (chiral C), 112.67 (Ar), 114.00 (Ar), 115.34 (Ar), 116.46 (Ar), 118.87 (two peaks, Ar), 119.45 (Ar), 121.33 (Ar), 125.67 (Ar), 126.23 (Ar), 128.98
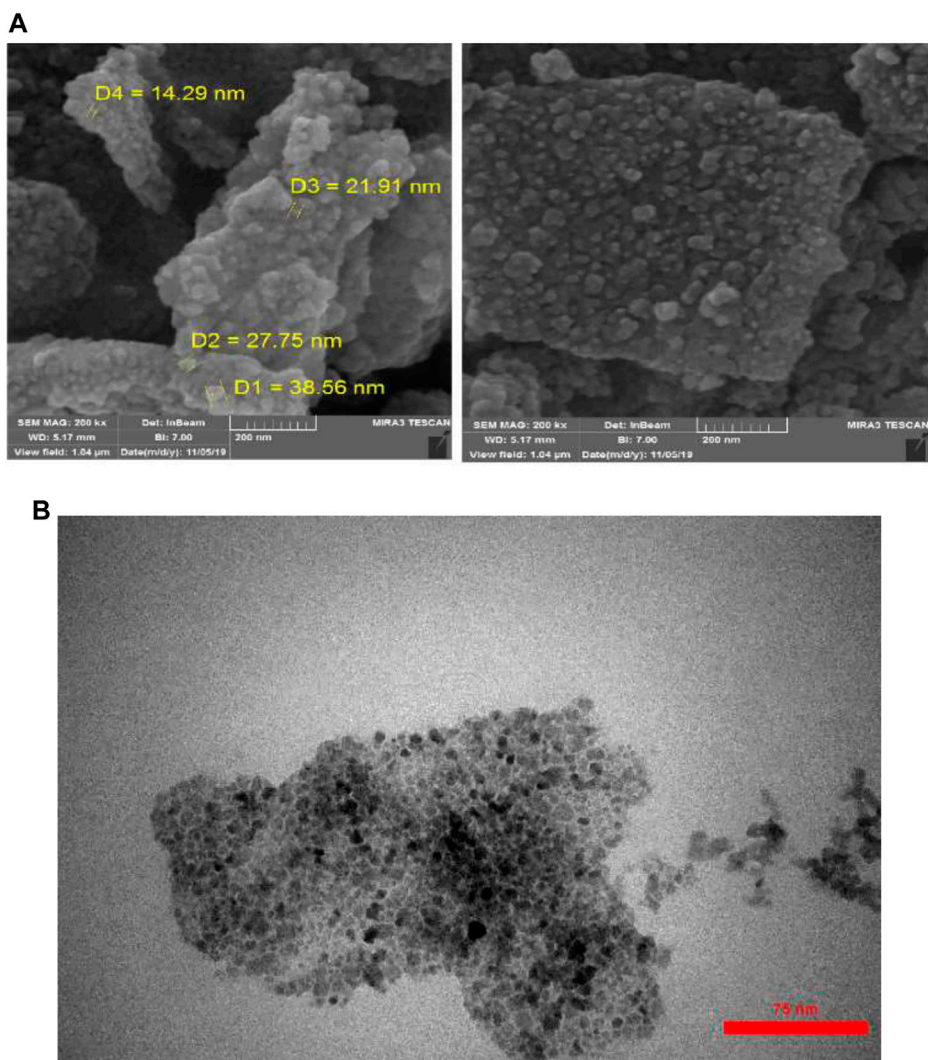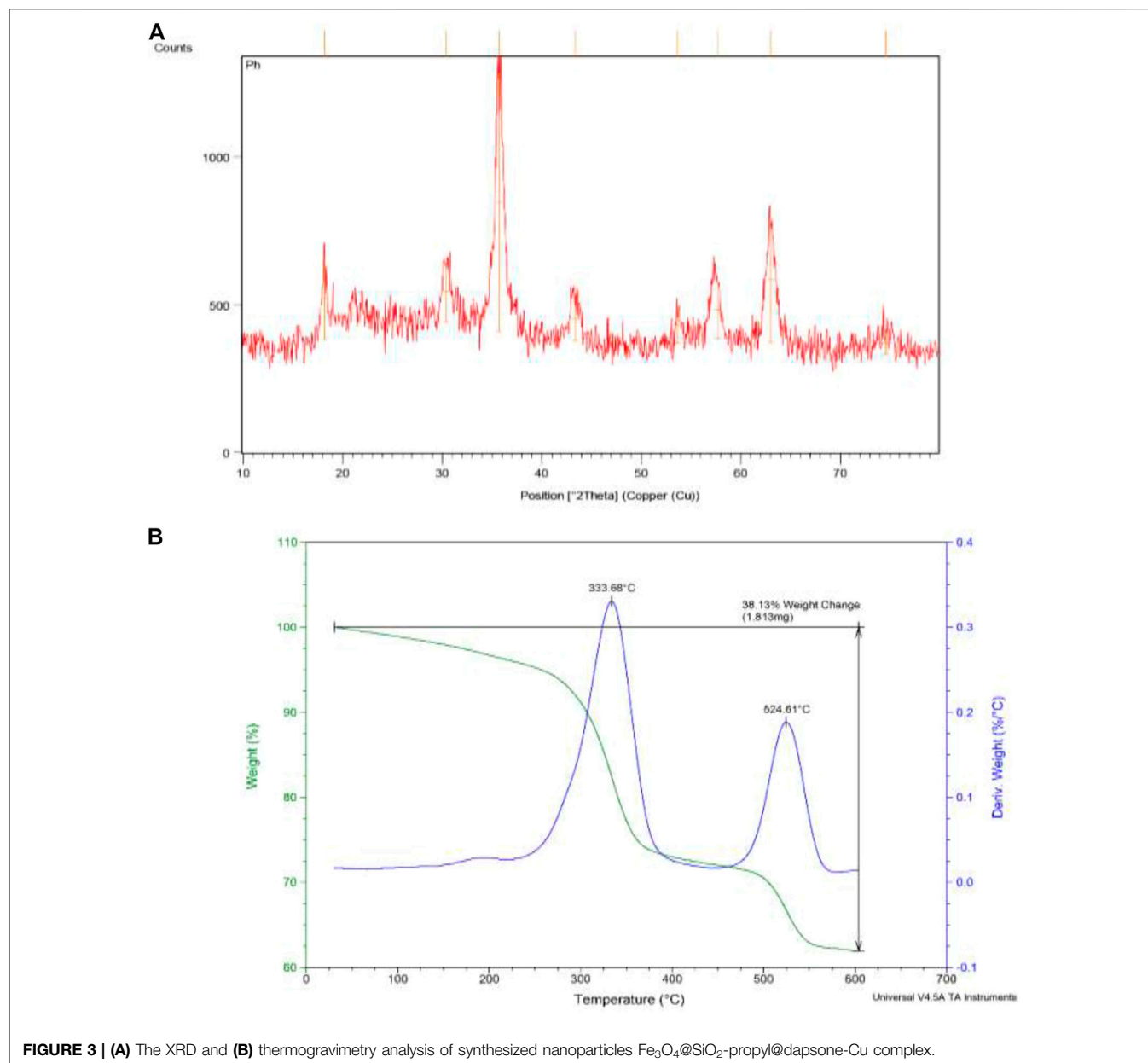
FIGURE 1 | (A) FE-SEM and **(B)** TEM images of synthesized Fe$_3$O$_4$@SiO$_2$-pr@dapsone-Cu.

FIGURE 2 | FT-IR spectra of Fe$_3$O$_4$@SiO$_2$-propyl@dapsone-Cu MNPs.

FIGURE 3 | (A) The XRD and **(B)** thermogravimetry analysis of synthesized nanoparticles Fe_3O_4@SiO_2-propyl@dapsone-Cu complex.

(Ar), 129.00 (two peaks, Ar), 132.46 (Ar), 135.47 (Ar), 135.88 (Ar), 137.98 (Ar), 141.12 (Ar), 143.34 (Ar), 146.54 (Ar), 198.08 (C=O), 200.23 (C=O) ppm. Anal. Calcd. for $C_{26}H_{16}O_4$: C, 79.58; H, 4.11. Found: C, 79.53; H, 4.07.

RESULT AND DISCUSSION

Synthesis and Characterization

In order to prepare nanocatalyst, initially, Fe3O4 MNPs were modified with silica and then with chloropropyl silane via chemical bonds to obtain Fe3O4@SiO2-pr. In the next step, Fe3O4@SiO2-propyl was covalent by substitution reaction by dapsone to prepare Fe3O4@SiO2-propyl loaded dapsone.

This nanocatalyst was treated with copper chloride to produce Fe3O4@SiO2-propyl@dapsone-Cu (**Scheme 1**). The structure of the prepared nanocatalyst was studied and fully characterized using FT-IR, energy-dispersive X-ray (EDX), XRD, zeta potential, TEM, and field emission scanning electron microscope (FE-SEM) analysis.

As shown in **Figure 1** (FE-SEM and TEM), the magnetic nanoparticles have a spherical shape with an average diameter of 14–38 nm. The synthesized nanoparticles have aggregated well.

Figure 2 shows FT-IR spectra of Fe_3O_4@SiO_2-propyl@ dapsone-Cu MNPs. Wavenumbers of Fe-O bonds of Fe_3O_4 appear in 569 and 467 cm^{-1} in Fe_3O_4@SiO_2-propyl@dapsone-Cu MNPs. The peaks positioned at 2,928 cm^{-1} are assigned to
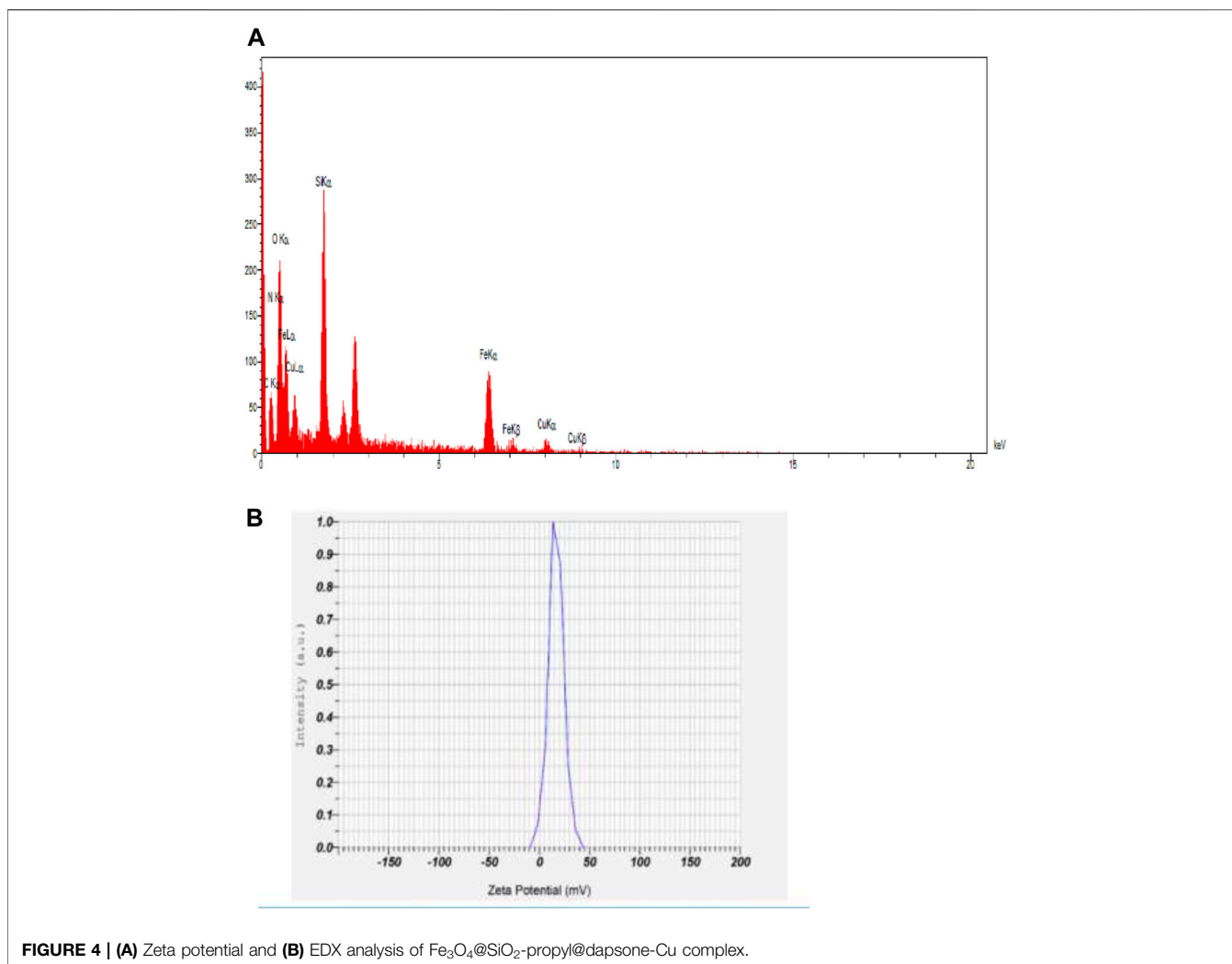
FIGURE 4 | **(A)** Zeta potential and **(B)** EDX analysis of Fe_3O_4@SiO_2-propyl@dapsone-Cu complex.

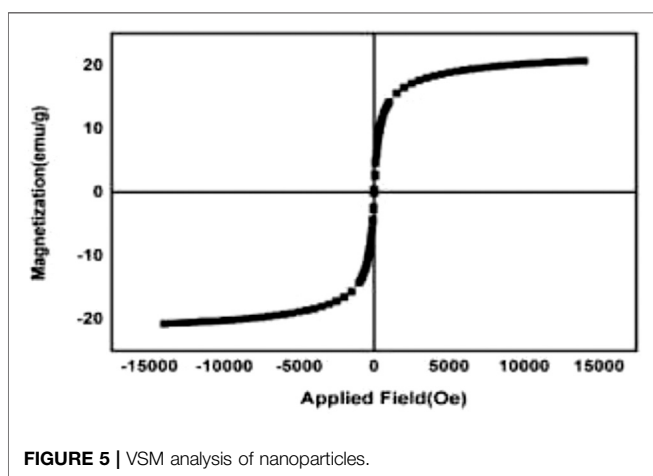FIGURE 5 | VSM analysis of nanoparticles.

aliphatic C-H bonds of Fe_3O_4@SiO_2-propyl@dapsone-Cu MNPs. The peak at 1,102 cm^{-1} and 1,141 cm^{-1} is attributed to Si-O-Si stretching modes of Fe_3O_4@SiO_2-propyl@dapsone-Cu.

Furthermore, the other peaks were seen as 1,594 (S=O stretching), 1,628 (aromatic C=C stretching), 3,371 (N-H stretching), and 1,343 cm^{-1} (C-N stretching) in Fe_3O_4@SiO_2-propyl@dapsone-Cu.

The XRD pattern of synthesized nanoparticles showed the sharp diffraction peaks with 2θ at 18° (111), 30.4° (220), 35.7° (311), 43.3° (400), 53.6° (422), 57.7° (511), 63.0° (440), and 74.6 (533) (**Figure 3A**), which indicate that the MNPs have highly crystalline cubic spinel structure of the magnetite and matched with the diffraction patterns of the standard Fe_3O_4 (JCPD 19–0629). This confirmed the stability of the crystalline phase of the magnetite core in the structure after silica coating, condensation, and complexation process. The absence of an amorphous peak in pattern confirmed the crystalline structure. Using *Debye–Scherrer equation*, the mean size of crystallite was calculated as 12.1 nm from the XRD pattern (crystallite shape factor: 0.9 and λ_{CuKa1} = 1.54060 Å). This value is lower than the size obtained by FE-SEM and TEM due to the fact that some crystallite forms a particle. Also, the d-spacing and full width at half maximum
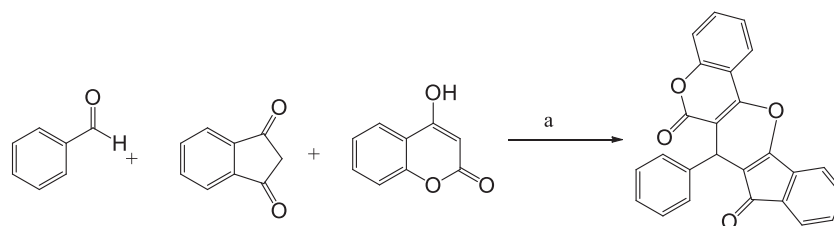
a: Fe3O4@SiO2-propyl@dapsone-Cu , distilled water

SCHEME 2 | Multicomponent synthesis of pyrano[3,2-c]chromene-diones.

TABLE 1 | The optimization reaction conditions for the synthesis of 4a.

Catalyst	Condition	Time (h)	Yield (%)
—	Refluxing in EtOH	48	11
HCl (concentrated)	Refluxing in EtOH, 10drops	48	28
AcOH	Refluxing in EtOH, 0.1 ml	48	35
K10	Refluxing in EtOH, 0.1 g	24	45
HY-zeolite	Refluxing in EtOH, 0.1 g	24	51
DBU-Ac	Heating at 90°C, 0.5 ml	30	43
DABCO-diAc	Heating at 90°C, 0.5 ml	26	47
Nano-Fe_3O_4	Refluxing in EtOH, 0.1 g	12	58
Fe_3O_4@SiO_2	Refluxing in EtOH, 0.1 g	6	62
Fe_3O_4@SiO_2-pr	Refluxing in EtOH, 0.1 g	6	64
Fe_3O_4@SiO_2-Pr@dapsone	Refluxing in EtOH, 0.1 g	5	73
Fe_3O_4@SiO_2-propyl@dapsone-Cu	Refluxing in EtOH, 0.1 g	3	97
Fe_3O_4@SiO_2-propyl@dapsone-Cu	Refluxing in EtOH, 0.01 g	6	76
Fe_3O_4@SiO_2-propyl@dapsone-Cu	Refluxing in EtOH, 0.05 g	3	96
Fe_3O_4@SiO_2-propyl@dapsone-Cu	Stirring at room temperature in water, 0.05 g	3	98

(FWHM) of the highest XRD peak (2θ = 35.71°) were obtained as 2.514 Å and 0.6888 (2θ°).

Figure 3B revealed the TGA analysis of synthesized nanoparticles. Two weight losses are observed. The first decrease is related to a temperature below 333°C because of desorption of water and the second weight-loss step at 524°C is due to decomposition of organic compound as dapsone.

As shown in **Figure 4A**, the zeta potential was scanned. The large zeta potential obtained revealed a more stable dispersion of synthesized MNPs. The zeta potential value of dispersed synthesized in deionized water in absence of any electrolyte was +25.1 mV.

The presence of iron, oxygen, nitrogen, carbon, silica, sulfur, and copper, in EDX, revealed the successful synthesis of these nanoparticles.

The magnetic properties of synthesized nanoparticles are shown in **Figure 5**. The results approve the superparamagneticity behavior.

Catalytic Application

In continuation of our study to synthesize pharmaceutical compounds (Fekri et al., 2018a, b; Fekri and Fard, 2016; Zare et al., 2010; Nikpassand et al., 2012; Fekri and Nikpassand 2014), we triggered to use Fe_3O_4@SiO_2-propyl@dapsone-Cu nanoparticles, for the multicomponent synthesis of novel derivatives of pyrano[3,2-c]

chromene-diones via the multicomponent reaction between various aldehydes, indan-1,3-dione, and 4-hydroxycoumarine (**Scheme 2**).
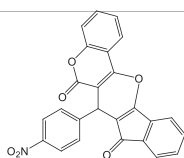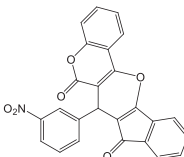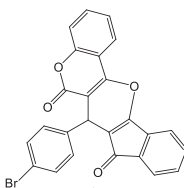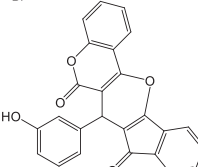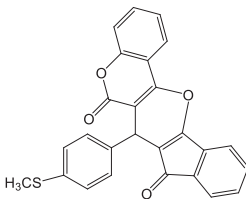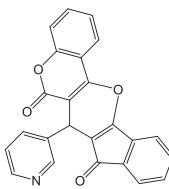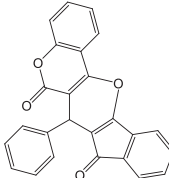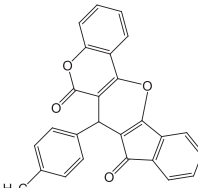
To complete our assessment, we checked the effect of different conditions in the sample reaction. For example, we treated 4-nitrobenzaldehyde, indandione, and 4-hydroxycoumarin under stirring at room temperature and refluxing in EtOH. The satisfactory results were obtained via the reaction of 4-nitrobenzaldehyde, indandione, and 4-hydroxycoumarin in the presence of 0.05 g of Fe_3O_4@SiO_2-propyl@dapsone-Cu in aqueous media under stirring (**Table 1**).

To expand the generality and efficiency of this avenue, some aldehydes with electron-donating or electron-withdrawing substituents were treated with indan-1,3-dione and 4-hydroxycoumarin. The results are summarized in **Table 2**.

As a proposed mechanistic pathway, initially, aldehyde was activated by the nanocatalyst, followed by nucleophilic attack of C-H acid of indan-1,3-diones, together with the departure of water, and chalcone was produced. Nucleophilic attack of 4-hydroxycoumarin to chalcone as Michael addition and then intramolecular cyclization followed by elimination of water lead to product 4 (**Scheme 3**).

Furthermore, the magnetic nanoparticles are magnetically recoverable and can be reused for six runs. Appearance

TABLE 2 | The reaction scope of synthesis of pyrano[3,2-c]chromene-diones.

Entry	Product	Time (h)	Yield (%)[a,b]	Mp (°C)
1		3	98	203–205
2		3	96	176–177
3		3.5	97	276–278
4		4	94	289–290
5		4	95	269–270
6		4	96	>300
7		5	94	203–205
8		5.5	90	234–235

[a]Isolated yield.
[b]All of the synthesized compounds are new and are characterized by FT-IR, NMR, and elemental analysis.
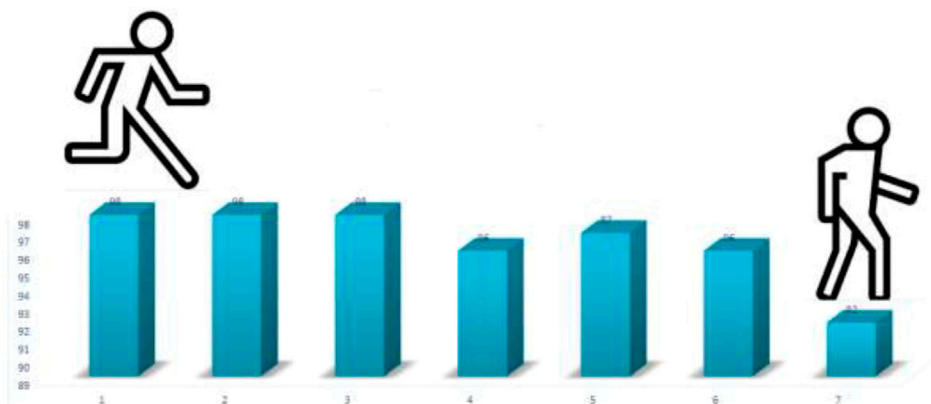
FIGURE 6 | The recyclability of nanocatalyst.

pathway a)

This intermediate has contineous resonance and is preferable

pathway b)

This intermediate has cross resonance
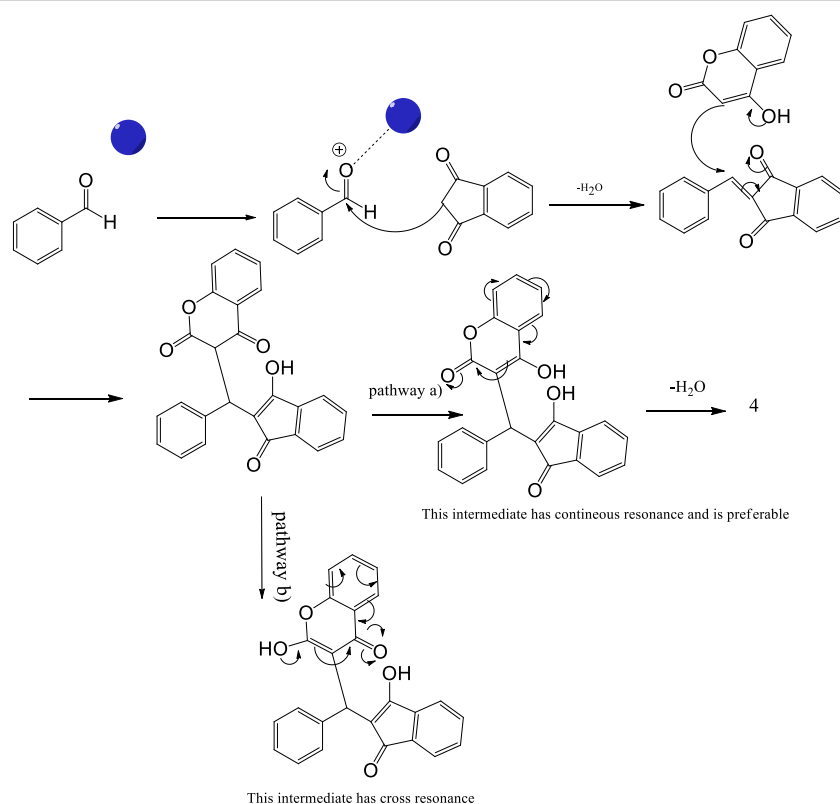
SCHEME 3 | Proposed mechanism for the synthesis of pyranochromene-diones.

features of the catalyst were not changed after several uses (**Figure 6**).

To better understand the stability of catalyst after five cycles under these reaction conditions, FE-SEM and TEM analyses were carried out. The results are summarized in **Figure 7**.

CONCLUSION

In conclusion, a new catalytic method for the synthesis of pyrano [3,2-c]chromene-diones has been developed. This method offers several advantages, such as simple workup and purification procedure without the use of any chromatographic method,
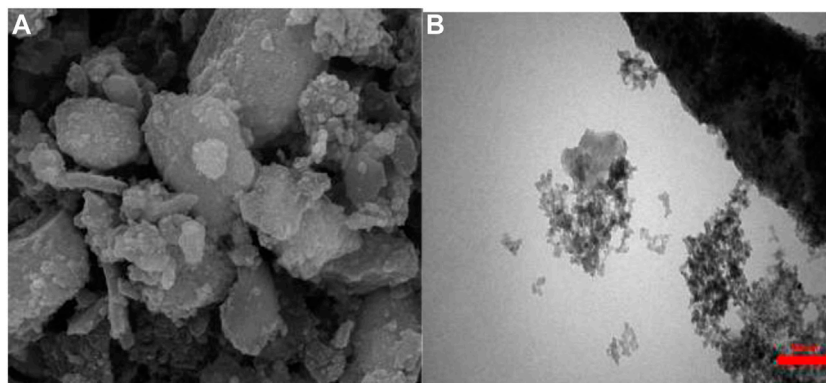
FIGURE 7 | (A) FE-SEM and **(B)** TEM image of reused synthesized catalyst in the sixth run.

mild reaction conditions, use of inexpensive and commercially available starting materials, recyclability and reusability of the catalyst, high product yields, and short reaction time. So we think that this procedure could be considered a new and useful addition to the present methodologies in this area.

DATA AVAILABILITY STATEMENT

The original contributions presented in the study are included in the article/supplementary files, further inquiries can be directed to the corresponding author.

REFERENCES

AUTHOR CONTRIBUTIONS

LZ carried out experimental studies, wrote the original draft, and analyzed spectral characterization of synthesized molecules and project planning, proofreading, and editing.

Abbasi, Z., Rezayati, S., Bagheri, M., and Hajinasiri, R. (2017). Preparation of a Novel, Efficient, and Recyclable Magnetic Catalyst,γ-Fe₂O₃@HAp-Ag Nanoparticles, and a Solventand Halogen-free Protocol for the Synthesis of Coumarin Derivatives. *Chin. Chem. Lett.* 28, 75–82. doi:10.1016/j.cclet.2016.06.022

Barnard, D. L., Xu, Z. Q., Stowell, V. D., Yuan, H., Smee, D. F., Samy, R., et al. (2002). Coumarins and Pyranocoumarins, Potential Novel Pharmacophores for Inhibition Ofmeasles Virus Replication. *Antivir. Chem. Chemother.* 17, 39–59. doi:10.1177/095632020201300104

Bienaymé, H., Hulme, C., Oddon, G., and Schmitt, P. (2000). Maximizing Synthetic Efficiency: Multi-Component Transformations lead the Way. *Chem. Eur. J.* 6, 3321–3329. doi:10.1002/1521-3765(20000915)6:18<3321:aid-chem3321>3.0.co;2-a

Dömling, A. (2002). Recent Advances in Isocyanide-Based Multicomponent Chemistry. *Curr. Opin. Chem. Biol.* 6, 306–313. doi:10.1016/S1367-5931(02)00328-9

Dömling, A., and Ugi, I. (2000). Multicomponent Reactions with Isocyanides. *Angew. Chem. Int. Ed.* 39, 3168–3210. doi:10.1002/1521-3773(20000915)39:18<3168:AID-ANIE3168>3.0

Fekri, L. Z., and Fard, H. S. (2016). 1,4-Diazaniumbicyclo[2.2.2]octane Diacetate: As an Effective, New and Reusable Media for the Synthesis of 14-Aryl-14h-Dibenzo[a,j]xanthenes. *Acta Chim. Slov* 63, 263–270. doi:10.17344/acsi.2015.2096

Fekri, L. Z., and Maleki, R. (2017). KIT-6 Mesoporous Silica-Coated Magnetite Nanoparticles: A Highly Efficient and Easily Reusable Catalyst for the Synthesis of Benzo[d]imidazole Derivatives. *J. Hetero. Chem.* 54, 1167–1171. doi:10.1002/jhet.2686

Fekri, L. Z., Nikpassand, M., Pourmirzajani, S., and Aghazadeh, B. (2018a). Synthesis and Characterization of Amino Glucose-Functionalized Silica-Coated NiFe2O4

Nanoparticles: a Heterogeneous, New and Magnetically Separable Catalyst for the Solvent-free Synthesis of Pyrano[3,2-C]chromen-5(4h)-Ones. *RSC Adv.* 8, 22313–22320. doi:10.1039/C8RA02572J

Fekri, L. Z., Nikpassand, M., Shariati, S., Aghazadeh, B., and Zarkeshvari, R. (2018b). Synthesis and Characterization of Amino Glucose-Functionalized Silica-Coated NiFe₂O₄ Nanoparticles: A Heterogeneous, New and Magnetically Separable Catalyst for the Solvent-free Synthesis of 2,4,5–trisubstituted Imidazoles. *J. Orgmet. Chem.* 871, 60–73. benzo[d] imidazoles, benzo[d] oxazoles and azo-linked benzo[d]oxazoles. doi:10.1016/j.jorganchem.2018.07.008

Fekri, L. Z., and Nikpassand, M. (2014). Ultrasound-promoted Friedel-Crafts Acylation of Arenes and Cyclic Anhydrides Catalyzed by Ionic Liquid of [bmim]Br/AlCl3. *Russ. J. Gen. Chem.* 84, 1825–1829. doi:10.1134/S107036321409031X

Fekri, L. Z., Pour, K. H., and Zeinali, S. (2020). Synthesis, Characterization and Application of Copper/Schiff-Base Complex Immobilized on KIT-6-NH2 Magnetic Nanoparticles for the Synthesis of Dihydropyridines. *J. Organomet. Chem.* 915, 121232. doi:10.1016/j.jorganchem.2020.121232

Fekri, L. Z. (2020). s-Proline Covalented Silicapropyl Modified Magnetic Nanoparticles: Synthesis, Characterization, Biological and Catalytic Activity for the Synthesis of Thiazolidin-4- Ones. *Curr. Org. Synth.* 17, 464–472. doi:10.2174/1570179417666200430121809

Fekri, L. Z., and Zeinali, S. (2020). Copper/Schiff-base Complex Immobilized on Amine Functionalized Silica Mesoporous Magnetic Nanoparticles under Solvent-free Condition: A Facile and New Avenue for the Synthesis of Thiazolidin-4-ones. *Appl. Organometal Chem.* 34, e5629. doi:10.1002/aoc.5629

Grieco, P. A. (1998). *Organic Synthesis in Water*. London: Blackie Academic and Professional. doi:10.1007/978-94-011-4950-1

Hosseini-Zare, M. S., Mahdavi, M., Saeedi, M., Asadi, M., Javanshir, S., Shafiee, A., et al. (2012). Synthesis of 2, 3-Diaryl-5h-Imidazo [2, 1-a] Isoindol-5-Ones via the One-Pot Reaction of 1, 2-diketones, 2-formylbenzoic Acids, and

Ammonium Acetate. *Tetrahedron Lett.* 53, 3448–3451. doi:10.1016/j.tetlet.2012.04.088

Inaloo, I. D., EsmaeilpourMajnooni, M. S., and Oveisi, A. R. (2020a). Nickel-catalyzed Synthesis of *N*-(Hetero)aryl Carbamates from Cyanate Salts and Phenols Activated with Cyanuric Chloride. *Chem. Cat. Chem.* 12 (21), 5486–5491. doi:10.1002/cctc.202000876

Inaloo, I. D., Majnooni, S., Eslahi, H., and Esmaeilpour, M. (2020d). Air-Stable Fe₃O₄@SiO₂-EDTA-Ni(0) as an Efficient Recyclable Magnetic Nanocatalyst for Effective Suzuki-Miyaura and Heck. *Cross-coupling via aryl Sulfamates and Carbamates* 34, e5662. doi:10.1002/aoc.5662

Inaloo, I. D., Majnooni, S., Eslahi, H., and Esmaeilpour, M. (2020b). Efficient Nickel(II) Immobilized on EDTA-modified Fe₃O₄@SiO₂ Nanospheres as a Novel Nanocatalyst for Amination of Heteroaryl Carbamates and Sulfamates through the Cleavage of C-O Bond. *Mol. Catal.* 492, 110915. doi:10.1016/j.mcat.2020.110915

Inaloo, I. D., Majnooni, S., Eslahi, H., and Esmaeilpour, M. (2020c). *N*-arylation of (Hetero) Arylamines Using Aryl Sulfamates and Carbamates *via* C–O Bond Activation Enabled by a Reusable and Durable Nickel(0) Catalyst. *New J. Chem.* 44, 13266–13278. doi:10.1039/D0NJ01610A

Kandhasamy, K., and Gnanasambandam, V. (2009). Multi-component Reactions in Water. *Curr. Org. Chem.* 13, 1820–1841. doi:10.2174/138527209789630514

Kongkathip, B., Kongkathip, N., Sunthitikawinsakul, A., Napaswat, C., and Yoosook, C. (2005). Anti-HIV-1 Constituents fromClausena Excavata: Part II. Carbazoles and a Pyranocoumarin. *Phytother. Res.* 19, 728–731. doi:10.1002/ptr.1738

Kumar, A., Maurya, R. A., Sharma, S., Ahmad, P., Singh, A. B., Bhatia, G., et al. (2009). Pyranocoumarins: a New Class of Anti-hyperglycemic and Anti-dyslipidemic Agents. *Bioorg. Med. Chem. Lett.* 19, 6447–6451. doi:10.1016/j.bmcl.2009.09.031

Lee, H. J., Lee, H. J., Lee, E. O., Lee, J. H., Lee, K. S., Kim, K. H., et al. (2009). *In Vivo* Anti-Cancer Activity of Korean *Angelica Gigas* and its Major Pyranocoumarin Decursin. *Am. J. Chin. Med.* 37, 127–142. doi:10.1142/S0192415X09006722

Li, C. J., and Chan, T. H. (1997). *Organic Reactions in Aqueous media*. New York, NY, USA: Wiley.

Lima, V., Silva, C. B., Mafezoli, J., Bezerra, M. M., Moraes, M. O., Mourão, G. S. M. M., et al. (2006). Antinociceptive Activity of the Pyranocoumarin Seselin in Mice. *Fitoterapia* 77, 574–578. doi:10.1016/j.fitote.2006.09.005

Magiatis, P., Melliou, E., Skaltsounis, A.-L., Mitaku, S., Léonce, S., Renard, P., et al. (1998). Synthesis and Cytotoxic Activity of Pyranocoumarins of the Seselin and Xanthyletin Series. *J. Nat. Prod.* 61, 982–986. doi:10.1021/np9800295

Mao, W.-w., Wang, T.-t., Zeng, H.-p., Wang, Z.-y., Chen, J.-p., and Shen, J.-g. (2009). Synthesis and Evaluation of Novel Substituted 5-hydroxycoumarin and Pyranocoumarin Derivatives Exhibiting Significant Antiproliferative Activity against Breast Cancer Cell Lines. *Bioorg. Med. Chem. Lett.* 19, 4570–4573. doi:10.1016/j.bmcl.2009.06.098

Mokhtary, M. (2016). Recent Advances in Catalysts Immobilized on Magnetic Nanoparticles. *J. Iran. Chem. Soc.* 13, 1827–1845. doi:10.1007/s13738-016-0900-4

Müller, T. J. J. (2014). *Science of Synthesis, Multicomponent Reactions I*. Stuttgart, New York: Georg Thieme Verlag KG.

Nikpassand, M., Fekri, L. Z., and Nabatzadeh, M. (2017). Fe3O4@SiO2@KIT-6 as an Efficient and Reusable Catalyst for the Synthesis of Novel Derivatives of 3,3'-((Aryl-1-Phenyl-1h-Pyrazol-4- Yl)methylene)bis (1H-Indole). *Comb. Chem.High. Throughput. Screen.* 20, 533–538. doi:10.2174/1386207320666170425123248

Nikpassand, M., Zare, L., and R. Mousavi, M. (2012). Comparative Study for the Aqeous Synthesis of New Generation of Diindolylmethanes Using L-Proline,

K10 and Nano-Fe3O4 under Ultrasound Irradiation. *Loc* 9 (5), 375–381. doi:10.2174/157017812801264719

Ouf, N. H., Selim, Y. A., Sakran, M. I., and Badr El-din, A. S. (2014). Synthesis of Pyranochromene and Pyranopyrimidine Derivatives from Substituted Natural Coumarin Isolated from Ammi Majus L. And Their Biological Evaluation. *Med. Chem. Res.* 23, 1180–1188. doi:10.1007/s00044-013-0724-z

Rezaee Nezhad, E., Sajjadifar, S., Abbasi, Z., and Rezayati, S. (2014). Chemoselective Synthesis of 1,1-diacetate Using Ni²⁺@hydroxyapatite-Core@shell γ-Fe₂O₃ Nanoparticles as an Efficient and Reusable lewis Acid Catalyst under Solvent Free Conditions. *J. Sci.* 25, 125–132.

Rezayati, S., Jafroudi, M. T., Nezhad, E. R., Hajinasiri, R., and Abbaspour, S. (2016). Imidazole-functionalized Magnetic Fe3O4 Nanoparticles: an Efficient, green, Recyclable Catalyst for One-Pot Friedländer Quinoline Synthesis. *Res. Chem. Intermed* 42, 5887–5898. doi:10.1007/s11164-015-2411-9

Sardarian, A. R., Dindarloo Inaloo, I., and Zangiabadi, M. (2019). An Fe3O4@ SiO2/Schiff base/Cu(ii) Complex as an Efficient Recyclable Magnetic Nanocatalyst for Selective Mono N-Arylation of Primary O-Alkyl Thiocarbamates and Primary O-Alkyl Carbamates with Aryl Halides and Arylboronic Acids. *New J. Chem.* 43, 8557–8565. doi:10.1039/C9NJ00028C

Su, C.-R., Yeh, S. F., Liu, C. M., Damu, A. G., Kuo, T.-H., Chiang, P.-C., et al. (2009). Anti-HBV and Cytotoxic Activities of Pyranocoumarin Derivatives. *Bioorg. Med. Chem.* 17, 6137–6143. doi:10.1016/j.bmc.2008.12.007

Symeonidis, T., Fylaktakidou, K. C., Hadjipavlou-Litina, D. J., and Litinas, K. E. (2009). Synthesis and Anti-inflammatory Evaluation of Novel Angularly or Linearly Fused Coumarins. *Eur. J. Med. Chem.* 44, 5012–5017. doi:10.1016/j.ejmech.2009.09.004

Williams, R. M., and Cox, R. J. (2003). Paraherquamides, Brevianamides, and Asperparalines: Laboratory Synthesis and Biosynthesis. An Interim Report. *Acc. Chem. Res.* 36, 127–139. doi:10.1021/ar020229e

Xu, Z.-Q., Pupek, K., Suling, W. J., Enache, L., and Flavin, M. T. (2006). Pyranocoumarin, a Novel Anti-TB Pharmacophore: Synthesis and Biological Evaluation against *Mycobacterium tuberculosis*. *Bioorg. Med. Chem.* 14, 4610–4626. doi:10.1016/j.bmc.2006.02.017

Zare, L., Mahmoodi, N. O., Yahyazadeh, A., Mamaghani, M., and Tabatabaeian, K. (2010). An Efficient Chemo- and Regioselective Three-Component Synthesis of Pyridazinones and Phthalazinones Using Activated KSF. *Chin. Chem. Lett.* 21, 538–541. doi:10.1016/j.cclet.2009.11.032

Zhang, G., Zhang, Y., Yan, J., Chen, R., Wang, S., Ma, Y., et al. (2012). One-pot Enantioselective Synthesis of Functionalized Pyranocoumarins and 2-Amino-4*h*-Chromenes: Discovery of a Type of Potent Antibacterial Agent. *J. Org. Chem.* 77, 878–888. doi:10.1021/jo202020m

Conflict of Interest: The authors declare that the research was conducted in the absence of any commercial or financial relationships that could be construed as a potential conflict of interest.

Publisher's Note: All claims expressed in this article are solely those of the authors and do not necessarily represent those of their affiliated organizations, or those of the publisher, the editors and the reviewers. Any product that may be evaluated in this article, or claim that may be made by its manufacturer, is not guaranteed or endorsed by the publisher.